Babol University Of Medical Sciences

IJMCM, Spring 2025, VOL 14, NO 2

International Journal of Molecular and Cellular Medicine

Journal homepage: www.ijmcmed.org

ORGINAL ARTICLE

Evaluation of the Antibacterial and Anti-Biofilm Activity of Chitosan-Arginine Nanoparticles and Sodium Fluoride against *Streptococcus mutans*

Fahimeh Daneshyar[1], Mohammad Yousef Alikhani[2], Soudeh Tayebi[1], Delaram Abedi Firouzjaei[1*]

1. Department of Pediatric dentistry, Faculty of Dentistry, Hamadan University of Medical Sciences, Hamadan, Iran
2. Infectious Disease Research Center, Avicenna Institute of Clinical Sciences, Hamadan University of Medical Sciences, Hamadan, Iran

ARTICLEINFO

Received: 2024/12/28
Revised: 2025/03/1
Accepted: 2025/03/3
DOI:

***Corresponding**:
Delaram Abedi Firouzjaei
Address:
Department of Pediatric dentistry, Faculty of Dentistry, Hamadan University of Medical Sciences, Hamadan, Iran
E-mail:
abedidelaram@yahoo.com

ABSTRACT

Dental caries is among the most prevalent chronic diseases. It arises from bacterial biofilm formation on tooth surfaces due to metabolic activity. *Streptococcus mutans* (*S. mutans*) is a key pathogen implicated in the development of dental caries. As bacterial resistance to conventional treatments increases, there is a growing interest in using novel compounds that possess antibacterial and antibiofilm properties. This study evaluated the effect of chitosan-arginine nanoparticles (CS-Arg NPs) and sodium fluoride (NaF) on inhibiting *S. mutans*' growth. After synthesizing CS-Arg NPs, their size, morphology, and chemical structure were evaluated. The broth microdilution method determined the minimum inhibitory concentration (MIC) and minimum bactericidal concentration (MBC) of CS-Arg NPs and NaF. The combined antibacterial and antibiofilm effect of CS-Arg NPs and NaF was assessed using the checkerboard method. The CS-Arg NPs had an average size of 269.9 nm with a zeta potential of +38.3 mV. The MIC of *S. mutans* for CS-Arg NPs and NaF was 312 µg/mL and 625 µg/mL, respectively, and the MBC for these NPs and NaF was 625 µg/mL and 2500 µg/mL, respectively. The fractional inhibitory concentration index (FICI) of the combination of CS-Arg NPs and NaF showed an additive effect (FICI = 1). The inhibitory effect of different concentrations of CS-Arg NPs and NaF, alone or in combination, on biofilm formation in the studied strain ranged from approximately 12% to 81%. This study demonstrated that CS-Arg NPs have antibacterial and antibiofilm properties against *S. mutans*, and their combination with NaF can enhance these antibacterial effects. These findings suggest that CS-Arg NPs and NaF, as a novel combination, could effectively develop oral hygiene products.

Keywords: Chitosan; Arginine; Sodium fluoride; *Streptococcus mutans*

Introduction

Oral diseases, especially dental caries, are among the most common global health issues, significantly affecting quality of life and imposing economic burdens (1). According to the Global Burden of Disease Study, untreated dental caries affects approximately 3.1 billion individuals worldwide, making it the most common chronic condition (2). Identifying caries risk factors is crucial in the epidemiology and clinical practice, as it informs the development of effective preventive strategies at individual and population levels (3).

Streptococcus mutans (*S. mutans*) primarily contribute to dental caries, forming biofilms on tooth surfaces and producing acids that demineralize enamel (4). Its ability to metabolize sugars, tolerate acidic conditions, and produce extracellular polysaccharides (EPS) enhances its cariogenic potential (5). Therefore, controlling *S. mutans*, particularly its biofilm form, is crucial in this regard. Traditional approaches to managing dental caries have focused on mechanically removing plaque through regular brushing and flossing (6). However, the rise of antimicrobial resistance among oral bacteria and the need for more effective and targeted treatments have driven research into alternative strategies. Incorporating novel antimicrobial agents into dental care products has emerged as a promising approach to enhance their efficacy against cariogenic bacteria (7). Chitosan (CS), a biopolymer derived from chitin, has recently been a research focus due to its biocompatibility, biodegradability, and antimicrobial properties (8). CS effectively prevents the formation and adhesion of dental plaque and biofilms by leveraging its positive charges to disrupt bacterial cell membranes, thereby inhibiting bacterial growth (9). CS-based nanoparticles (NPs) exhibit enhanced antibacterial activity compared to pure CS owing to their increased surface area and improved adhesion properties (9, 10). These benefits have made chitosan nanoparticles a promising option for preventing and treating dental caries. The amino acid L-arginine (Arg) plays a multifaceted role in the oral microbiome by inhibiting bacterial coaggregation, participating in cell-cell signaling, and altering bacterial metabolism across various species in the human oral cavity (11). Its use has shown potential in preventing the formation of cariogenic dental plaque biofilms (12). Research into the mechanism of action of Arg has primarily focused on its catabolism by oral streptococci, which increases local pH, effectively neutralizing the harmful effects of acid on teeth (13). Sodium fluoride (NaF) is the most widely utilized caries-preventive agent and is a key component in numerous oral care products (14). However, the emergence of fluoride-resistant *S. mutans* strains requires new formulations to improve its effectiveness. Combining chitosan-arginine (CS-Arg) NPs and NaF may offer a novel antibacterial strategy targeting multiple bacterial survival mechanisms (15, 16). This study aimed to synthesize CS-Arg NPs and evaluate their antibacterial and anti-biofilm effects against *S. mutans*, individually and in combination with sodium fluoride. This research explored an innovative approach to enhancing fluoride efficacy by modifying CS with Arg, contributing to the development of more effective oral care solutions.

Methods

Synthesis of Chitosan-Arginine (CS-Arg) Nanoparticles (NPs)

Low-molecular-weight chitosan (CS; Sigma, USA) was modified with arginine (Arg; Merck, Germany) using a previously established method with slight modifications (17). In summary, CS was dissolved in 1% acetic acid to create a uniform aqueous solution at room temperature. N-hydroxysuccinimide (NHS; Sigma, USA) was introduced into the solution at a 0.55 mol/mol EDC molar ratio under vigorous magnetic stirring. This was followed by adding 1-(3-dimethylaminopropyl)-3-ethylcarbodiimide (EDC; Sigma, USA) at a 1.5 mol/mol Arg molar ratio. Arg was then dissolved into the mixture and allowed to react under continuous stirring for 24 hours at ambient temperature. The resulting product underwent purification via dialysis against distilled water for three days and was ultimately recovered as freeze-dried CS-Arg NPs after 24 hours of lyophilization.

Characterization of CS-Arg NPs

The morphology and size of the CS-Arg NPs were characterized using a scanning electron microscope (SEC model SNE-4500, Korea). Dynamic light scattering (DLS, Microtrac NANOTRAC WAVE II) was utilized to determine the zeta potential and particle size. Fourier transform infrared spectroscopy (FTIR, Agilent Cary 630, USA) was employed to identify the

functional groups of the nanoparticles, with spectra recorded over a wavelength range of 400–4000 cm□¹.

Preparation of Sodium Fluoride (NaF)

This study used sodium fluoride (NaF; Sigma 106441). A stock solution was prepared by dissolving 50 mg of NaF in 10 mL of distilled water and filtering it through a 0.22 µm pore size membrane filter.

Bacterial Strain and Growth Conditions

This study used *S. mutans* PTCC 1683, obtained from the Iranian Biological Resources Center (Tehran, Iran). The bacterial strain was routinely grown under static conditions at 37°C in BHI broth.

Evaluation of Antibacterial Activity

The broth microdilution method determined the Minimum Inhibitory Concentration (MIC) and Minimum Bactericidal Concentration (MBC) of CS-Arg NPs and NaF against *S. mutans* (18). A bacterial suspension was standardized to 0.5 McFarland, diluted to 5×10^5 CFU/mL, and added to a 96-well plate containing Mueller-Hinton broth (MHB). Antibacterial solutions were serially diluted across columns 1–10, while columns 11 and 12 served as positive (bacteria with MHB) and negative (MHB only) controls, respectively. After adding 10 µL of bacterial suspension to all wells except the negative control, the plate was incubated at 37°C for 18–24 hours. MIC was determined as the lowest concentration at which bacterial growth was completely inhibited. The MBC was determined by inoculating cultures from wells where no bacterial growth was observed. An amount of 10 µL of the suspension from these wells was transferred onto Mueller-Hinton agar (MHA) plates, which were incubated at 37 °C for 24 hours. The MBC was defined as the lowest concentration of the antibacterial agent that killed 99.9% of the bacterial population.

Synergistic Impacts of Combining CS-Arg NPs with NaF

The Checkerboard method was used to investigate the antimicrobial effect of combining CS-Arg NPs and NaF (18). Briefly, a 96-well microtiter plate was used, where the rows contained two-fold serial dilutions of CS-Arg NPs ranging from 2500 to 2 µg/mL along the y-axis, and the columns contained two-fold serial dilutions of NaF ranging from 2500 to 39 µg/mL along the x-axis. The combined effects of CS-Arg NPs and NaF were evaluated using the fractional inhibitory concentration (FIC) index. This index was calculated using the formula: FIC index = FIC_A + FIC_B = (MIC of antimicrobial A in combination/MIC of A alone) + (MIC of antimicrobial B in combination/MIC of B alone). The interaction was categorized as synergistic if the FIC index was ≤0.5, additive if >0.5 and ≤1, indifferent if >1.0 and ≤2, and antagonistic if >2 (19).

Inhibition of Biofilm Formation

The effect of CS-Arg NPs and NaF on *S. mutans* was evaluated using a microtiter plate assay (20). *S. mutans* (1 × 10□ CFU/200 µL) in BHI-sucrose was incubated at 37°C for 24 hours in 96-well microtiter plates containing CS-Arg NPs and NaF at concentrations of 1× MIC, 1/2× MIC, 1/4× MIC, and 1/8× MIC. The positive control consisted of *S. mutans* in BHI-sucrose without any antimicrobial agents, while wells containing only BHI-sucrose medium served as the negative control. Following incubation, the supernatant was removed from each well, and the wells were washed three times with PBS.

For fixation, 200 µL of 99% methanol was added to each well and incubated for 15 minutes. Subsequently, the wells were stained with 200 µL of 0.1% crystal violet for 5 minutes. Excess dye was removed by washing with sterile distilled water. The biofilm-bound dye was then solubilized with 200 µL of 33% acetic acid for 15 minutes. Finally, each well's optical density (OD) was measured at 570 nm using an ELISA plate reader (Bio-Rad, USA).

The checkerboard method was employed to evaluate the synergistic anti-biofilm activity of CS-Arg NPs in combination with NaF (21). Initially, each isolate was inoculated into BHI with 2% sucrose and incubated at 37°C for 24 hours. A bacterial suspension was then prepared to a standard turbidity of 0.5 McFarland. This suspension was diluted 1:100 to achieve a final concentration of 10□ CFU/mL in a total volume of 200 µL.

Subsequently, 100 µL of the diluted suspension was added to the wells of a 96-well microplate containing 50 µL of various concentrations of the antimicrobial agents (CS-Arg NPs and NaF) at 4× MIC, ensuring that the final concentrations during incubation matched the MIC values upon mixing with the bacterial suspension and culture medium. The

microplate was incubated at 37°C for 24 hours. Following incubation, the biofilms were stained with crystal violet, as described, to measure the individual effects of substances on biofilm inhibition. Finally, the OD of each well was measured at 570 nm using an ELISA plate reader.

The percentage reduction in biofilm formation achieved with the studied combinations was calculated using the formula:

$$\text{Percentage of biofilm reduction} = \frac{\text{OD control} - \text{OD experimental}}{\text{OD control}} \times 100$$

Statistical Analysis

The data were analyzed using SPSS software, version 27. The data obtained from evaluating the anti-biofilm effects of the studied NPs against *S. mutans* were compared and analyzed using one-way analysis of variance (ANOVA). A p-value less than 0.05 was regarded as statistically significant.

Results

SEM Analysis

The morphology of CS-Arg NPs was analyzed using SEM, which showed that the nanoparticles possess an irregular and rough surface texture (Figure 1).

DLS Analysis

DLS analysis showed that the NPs had an average particle size of approximately 269.9 nm and a zeta potential of +38.3 mV (Figure 2).

FTIR Analysis

The FTIR spectrum of the CS-Arg NPs revealed various characteristic absorption bands, indicating the presence and interaction of functional groups. A broad band at 3258 cm^{-1} corresponds to overlapping O-H and N-H stretching vibrations, while bands at 2928 cm^{-1} and 2870 cm^{-1} are attributed to C-H stretching in CH_2 and CH_3 groups from CS and Arg. The carbonyl (C=O) stretching vibration of Arg's carboxylic acid appeared at 1653 cm^{-1} and shifted to lower wavelengths due to interactions with CS, while the amide carbonyl group of CS appeared at 1640 cm^{-1}. The C=N stretching vibration in arginine was observed at 1558 cm^{-1}, and bands at 1407 cm^{-1} and 1375 cm^{-1} corresponded to CH_2 and CH_3 bending vibrations. Additional bands included C-N amide stretching at 1313 cm^{-1} and C-O-C bridge and C-O stretching at 1152 cm^{-1}, 1060 cm^{-1}, and 1022 cm^{-1}. Notably, the N-H stretching band of primary amines in CS at 1589 cm^{-1} was absent, replaced by a new band at 1539 cm^{-1}, indicating NH_3^+ formation due to protonation in the acidic environment. The absence of the hydroxyl (-OH) band at 3050 cm^{-1}, typical of pure Arg, alongside shifts in the carbonyl band, confirmed acetylation and strong interactions between Arg and CS (Figure 3).

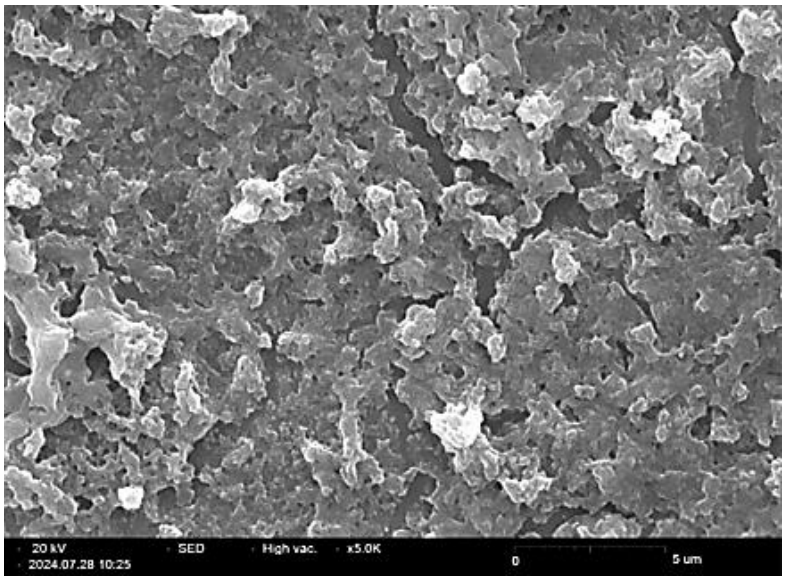

Figure 1. Morphological of chitosan-arginine nanoparticles (CS-Arg NPs). Scanning electron microscope (SEM) images depict CS-Arg NPs as having irregular and rough textures.

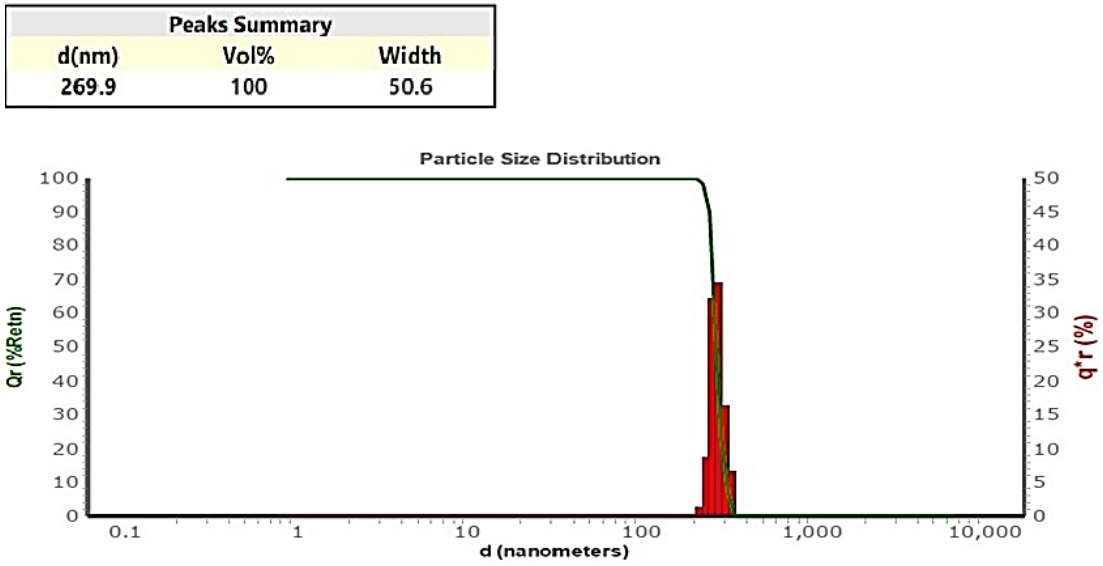

Figure 2. Size characterization of chitosan-arginine nanoparticles (CS-Arg NPs). Dynamic light scattering (DLS) analysis reveals an average particle size of 269.9 nm.

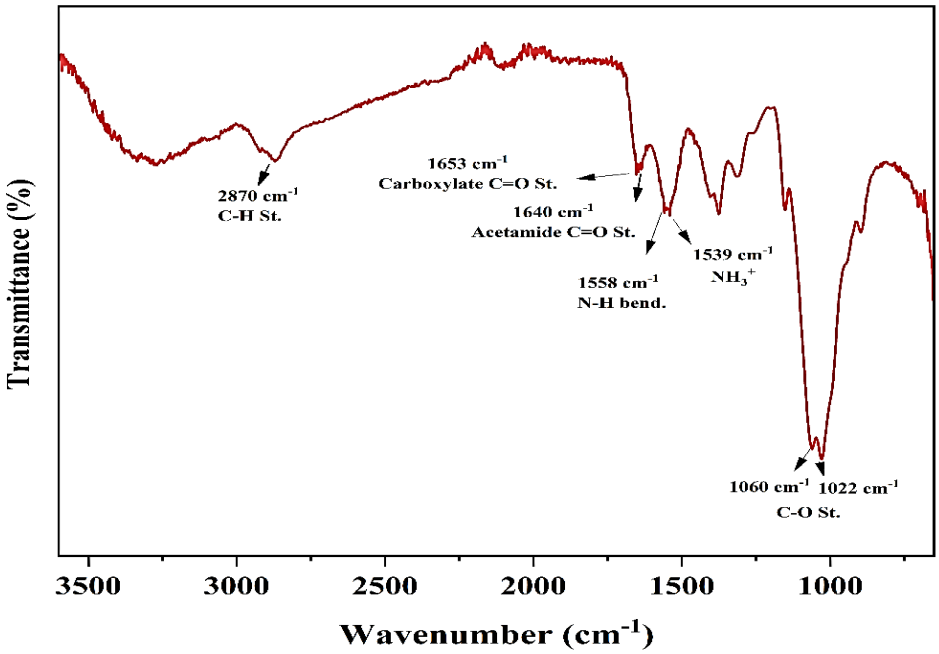

Figure 3. Fourier transform infrared spectroscopy (FTIR) spectrum of chitosan-arginine nanoparticles (CS-Arg NPs). The FTIR spectrum of CS-Arg NPs shows characteristic absorption bands, including O-H and N-H stretching at 3258 cm^{-1}, C=O stretching of arginine at 1653 cm^{-1} (shifted due to interaction with CS), and the absence of the CS primary amine band at 1589 cm^{-1}, replaced by NH_3^+ at 1539 cm^{-1}, confirming protonation. The disappearance of the -OH band at 3050 cm^{-1} and shifts in carbonyl bands suggest acetylation and strong CS-Arg NPs interactions.

Antibacterial Activity

The broth microdilution method determined the MICs of CS-Arg NPs and NaF. The MIC and MBC of CS-Arg NPs and NaF for *S. mutans* are presented in Table 1. These results indicated that the CS-Arg NPs exhibited more potent antibacterial activity against *S. mutans* than NaF.

FICI of CS-Arg NPs When Combined with NaF

The effects of CS-Arg NPs combined with NaF were evaluated using the checkerboard assay. The combination demonstrated additive effects against *S. mutans*, with a FICI of 1. The calculations for the FICI were as follows:

For CS-Arg NPs (A), FICA_AA = MIC of A in combination / MIC of A alone = 156/312 = 0.5.

For NaF (B), FICB_BB = MIC of B in combination / MIC of B alone = 312/625 = 0.5.

The FICI was calculated as FICA_AA + FICB_BB = 0.5 + 0.5 = 1, indicating an additive interaction.

Determination of Biofilm Formation Inhibitory Activity

As shown in Table 2, treatment with various concentrations of CS-Arg NPs and NaF reduced biofilm formation in *S. mutans*. The reduction in biofilm production was concentration-dependent, with higher concentrations of the antimicrobial agents resulting in more significant inhibition, while lower concentrations allowed more biofilm formation. The checkerboard method was used to assess the combined effects of CS-Arg NPs and NaF on *S. mutans* biofilm formation. The results (Table 2) demonstrated that combining these two antimicrobial agents was more effective at inhibiting biofilm formation than using either agent alone.

Table 1. MIC and MBC of chitosan-arginine nanoparticles (CS-Arg NPs) and sodium fluoride (NaF)

Compound	MIC (µg/mL)	MBC (µg/mL)
CS-Arg NPs	312	625
NaF	625	2500

Table 2. The effect of different concentrations of chitosan-arginine nanoparticles (CS-Arg NPs) and sodium fluoride (NaF) alone and in combination on the inhibition of biofilm formation in *S. mutans*

Compound	*S. mutans*					P-value
CS-Arg NPs	Concentrations (µg/mL)	312	156	78	39	0.07
	Biofilm inhibition (%)	66	58	32	12	
NaF	Concentrations (µg/mL)	625	312	156	78	0.085
	Biofilm inhibition (%)	73	64	41	15	
CS-Arg NPs + NaF	Concentrations (µg/mL)	312 + 625	156 + 312	78 + 156	39 + 78	0.097
	Biofilm inhibition (%)	81	67	49	27	

Discussion

This study evaluated the antibacterial and anti-biofilm efficacy of CS-Arg NPs and NaF against *S. mutans*, a primary contributor to dental caries, a prevalent global health issue. While effective, current oral care products have limitations, highlighting the need for innovative alternatives. CS exhibits notable antibacterial and anti-biofilm properties, which can be enhanced through modifications such as Arg conjugation to improve solubility and activity at physiological pH (22). Fluoride, a staple in oral care, prevents bacterial growth and tooth demineralization. Combining CS-Arg NPs with fluoride could synergistically address the dual challenges of biofilm formation and enamel protection, offering a promising strategy for dental caries prevention (23).

The properties of CS-Arg NPs in this study revealed findings regarding their size, surface charge, and functional groups, all contributing to their potential antibacterial and anti-biofilm effects against *S. mutans*. The average particle size, determined by DLS, was

269.9 nm, which is consistent with previous studies reporting similar or smaller sizes for CS-Arg NPs. For instance, Luo et al. identified CS-Arg NPs with an average size of approximately 75.76 nm (24). In contrast, Shikida et al. reported a mean size of about 274 nm for CS-Arg NPs (25). Variations in particle size could be attributed to differences in the molecular weight of the chitosan used or the specific synthesis methods employed. The zeta potential of the synthesized nanoparticles in this study was determined to be +38.3 mV, indicating a strongly positive surface charge. This suggests good colloidal stability and enhanced potential for interaction with negatively charged bacterial membranes. This finding is consistent with Mosaad et al.'s study, who reported that positively charged CS NPs had improved antibacterial activity due to their ability to disrupt bacterial cell membranes via electrostatic interactions (22). Similarly, Shikida et al. reported a zeta potential of +30 mV for synthesized CS-Arg NPs (25). The high zeta potential observed in this study supports the hypothesis that CS-Arg NPs effectively target *S. mutans*, and amplify their antibacterial efficacy. The FTIR analysis provided insights into the chemical structure of the NPs, confirming the successful incorporation of Arg into the CS matrix through peaks associated with amide bonds and carbonyl groups. These findings are consistent with previous research, such as Shikida et al., which demonstrated that CS NPs conjugated with Arg retained essential functional groups while enhancing their antimicrobial properties (25). Specific peaks identified in the FTIR spectrum, particularly those related to C-N and C-O-C vibrations, highlight that functional groups are critical for the antibacterial activity of CS derivatives.

This study determined the MIC and MBC values of CS-Arg NPs against *S. mutans* PTCC 1683 as 312 µg/mL and 625 µg/mL, respectively. The results indicated the superior efficacy of CS-Arg NPs in inhibiting and killing *S. mutans* compared to CS NPs. For instance, Valian et al. reported MIC values of 625–2500 µg/mL and MBC values of 1250–5000 µg/mL for CS NPs against *S. mutans* isolates (26). Similarly, Aliasghari et al. found MIC and MBC values of 625 µg/mL and 1250 µg/mL, respectively, for CS NPs against *S. mutans* ATCC 35668, demonstrating reduced efficacy compared to our findings (27). This improved antibacterial performance may be attributed to the unique properties of Arg when combined with chitosan, enhancing the NPs' effectiveness. This study determined the MIC and MBC values of NaF against *S. mutans* PTCC 1683 as 625 µg/mL and 2500 µg/mL, respectively. These findings are consistent with similar studies, such as Tong et al., who reported MIC and MBC values of 600 µg/mL and 3500 µg/mL for NaF against *S. mutans* UA159 (28), and Liu et al., who reported comparable values of 600 µg/mL and 2500 µg/mL (29). Variations in results, like the higher MBC reported by Cai et al. (625 µg/mL MIC and 5000 µg/mL MBC), may be attributed to differences in experimental conditions or the specific *S. mutans* strain used (30). Additionally, Melkam et al. noted a MIC of 500 µg/mL for *S. mutans* UA159 (31). This study demonstrated that CS-Arg NPs effectively inhibited biofilm formation in *S. mutans* PTCC 1683, with the extent of inhibition increasing at higher concentrations. These findings align with previous research showing that CS NPs exhibit anti-biofilm activity, even at relatively low concentrations (26).

Other studies have reported that CS NPs reduce biofilm formation, with greater efficiency observed at higher doses (27). Similarly, NaF treatment significantly reduced biofilm formation, reinforcing its well-documented role in preventing bacterial adhesion and growth. Earlier research has also demonstrated that NaF disrupts biofilms over time, highlighting its ability to weaken bacterial structures and reduce biofilm mass (29). This study demonstrated that combining varying concentrations of CS-Arg NPs and NaF enhanced their antibacterial and anti-biofilm effects against *S. mutans*. While the MIC was reduced in the combination, no synergistic interaction was observed. These findings align with Magalhaes et al., who highlighted the antibacterial and anti-biofilm efficacy of NaF-CS complexes. Fluoride ions inhibit enolase, essential for glucose metabolism, and ATP-dependent proton pumps, thereby reducing bacterial viability and growth. Additionally, the R-NH3□ groups in CS interact electrostatically with bacterial membranes, causing disruption. This combination optimizes the antibacterial properties of both agents, effectively reducing biofilm formation and enhancing therapeutic potential (32).

While this study provides valuable insights into the antibacterial and anti-biofilm effects of CS-Arg NPs and NaF, several limitations should be considered. As an in vitro study, the findings may not fully reflect the oral environment, requiring in vivo validation.

Additionally, only *S. mutans* PTCC 1683 was tested, while dental caries involve multiple bacteria, necessitating further research on multi-species biofilms. The precise molecular mechanisms of CS-Arg NPs and NaF also require deeper investigation. Lastly, optimizing the formulation, stability, and delivery method is essential for clinical application in oral care products.

The findings of this study indicated that both CS-Arg NPs and NaF exhibit effective antibacterial and anti-biofilm properties against *S. mutans*. While their combination reduced biofilm formation and inhibited bacterial growth, no synergistic effects were observed; only additive ones were noted. Nevertheless, this combination demonstrated significant potential for use in antibacterial formulations and could serve as an efficient strategy for managing oral infections and biofilm-resistant bacteria.

Funding

The study was funded by the Vice-Chancellery for Research and Technology, Hamadan University of Medical Sciences (No. 140204132868) and was approved by the Ethics Committee with the ethical code of IR.UMSHA.REC.1402.120.

References

1. Bawaskar HS, Bawaskar PH. Oral diseases: a global public health challenge. Lancet. 2020;395(10219):185-6.
2. Pitts NB, Twetman S, Fisher J, et al. Understanding dental caries as a non-communicable disease. Br Dent J. 2021;231(12):749-53.
3. Martignon S, Roncalli AG, Alvarez E, et al. Risk factors for dental caries in Latin American and Caribbean countries. Braz Oral Res. 2021;35(suppl 01):e053.
4. Matsumoto-Nakano M. Role of Streptococcus mutans surface proteins for biofilm formation. Jpn Dent Sci Rev. 2018;54(1):22-9.
5. Nguyen PT, Falsetta ML, Hwang G, et al. α-Mangostin disrupts the development of Streptococcus mutans biofilms and facilitates its mechanical removal. PLoS One. 2014;9(10):e111312.
6. Yang S, Zhang J, Yang R, et al. Small Molecule Compounds, A Novel Strategy against Streptococcus mutans. Pathogens. 2021;10(12):1540.
7. Rahman S, Sadaf S, Hoque ME, et al. Unleashing the promise of emerging nanomaterials as a sustainable platform to mitigate antimicrobial resistance. RSC Adv. 2024;14(20):13862-99.
8. Mawazi SM, Kumar M, Ahmad N, et al. Recent Applications of Chitosan and Its Derivatives in Antibacterial, Anticancer, Wound Healing, and Tissue Engineering Fields. Polymers (Basel). 2024;16(10):1351.
9. Rizeq BR, Younes NN, Rasool K, et al. Synthesis, Bioapplications, and Toxicity Evaluation of Chitosan-Based Nanoparticles. Int J Mol Sci. 2019;20(22):5776.
10. Gao H, Wu N, Wang N, et al. Chitosan-based therapeutic systems and their potentials in treatment of oral diseases. Int J Biol Macromol. 2022;222(Pt B):3178-94.
11. Kolderman E, Bettampadi D, Samarian D, et al. L-arginine destabilizes oral multi-species biofilm communities developed in human saliva. PLoS One. 2015;10(5):e0121835.
12. Nascimento MM, Browngardt C, Xiaohui X, et al. The effect of arginine on oral biofilm communities. Mol Oral Microbiol. 2014;29(1):45-54.
13. Gordan VV, Garvan CW, Ottenga ME, et al. Could alkali production be considered an approach for caries control? Caries Res. 2010;44(6):547-54.
14. Goyal V, Damle S, Puranik MP, et al. Arginine: A New Paradigm in Preventive Oral Care. Int J Clin Pediatr Dent. 2023;16(5):698-706.
15. Liao Y, Brandt BW, Li J, et al. Fluoride resistance in Streptococcus mutans: a mini review. J Oral Microbiol. 2017;9(1):1344509.
16. Bijle MNA, Ekambaram M, Lo EC, et al. The combined enamel remineralization potential of arginine and fluoride toothpaste. J Dent. 2018;7675-82.
17. Fu C, Qi Z, Zhao C, et al. Enhanced wound repair ability of arginine-chitosan nanocomposite membrane through the antimicrobial peptides-loaded polydopamine-modified graphene oxide. J Biol Eng. 2021;15(1):17.
18. Tong Z, Zhang Y, Ling J, et al. An in vitro study on the effects of nisin on the antibacterial activities of 18 antibiotics against Enterococcus faecalis. PLoS One. 2014;9(2):e89209.

19. Lee YS, Jang KA, Cha JD. Synergistic antibacterial effect between silibinin and antibiotics in oral bacteria. J Biomed Biotechnol. 2012;2012(2012):618081.
20. Mataraci E, Dosler S. In vitro activities of antibiotics and antimicrobial cationic peptides alone and in combination against methicillin-resistant Staphylococcus aureus biofilms. Antimicrob Agents Chemother. 2012;56(12):6366-71.
21. Rosato A, Sblano S, Salvagno L, et al. Anti-Biofilm Inhibitory Synergistic Effects of Combinations of Essential Oils and Antibiotics. Antibiotics (Basel). 2020;9(10):637.
22. Mosaad RM, Alhalafi MH, Emam EM, et al. Enhancement of Antimicrobial and Dyeing Properties of Cellulosic Fabrics via Chitosan Nanoparticles. Polymers (Basel). 2022;14(19):4211.
23. Marquis RE. Antimicrobial actions of fluoride for oral bacteria. Can J Microbiol. 1995;41(11):955-64.
24. Luo J, Chen J, Liu Y, et al. A Novel Form of Arginine-Chitosan as Nanoparticles Efficient for siRNA Delivery into Mouse Leukemia Cells. Int J Mol Sci. 2023;24(2):104
25. Shikida DNR, Dalmolin LF, Fumagalli F, et al. Arginine-conjugated chitosan nanoparticles for topical arginine release in wounds. J DRUG DELIV SCI TEC. 2021;61(1):1-8.
26. Valian A, Goudarzi H, Nasiri MJ, et al. Antibacterial and Anti-biofilm Effects of Chitosan Nanoparticles on Streptococcus Mutans Isolates. JIMC. 2023;6(2):292-8.
27. Aliasghari A, Rabbani Khorasgani M, Vaezifar S, et al. Evaluation of antibacterial efficiency of chitosan and chitosan nanoparticles on cariogenic streptococci: an in vitro study. Iran J Microbiol. 2016;8(2):93-100.
28. Tong Z, Zhou L, Jiang W, et al. An in vitro synergetic evaluation of the use of nisin and sodium fluoride or chlorhexidine against Streptococcus mutans. Peptides. 2011;32(10):2021-6.
29. Liu J, Ling JQ, Zhang K, et al. Effect of sodium fluoride, ampicillin, and chlorhexidine on Streptococcus mutans biofilm detachment. Antimicrob Agents Chemother. 2012;56(8):4532-5.
30. Cai JN, Kim MA, Jung JE, et al. Effects of combined oleic acid and fluoride at sub-MIC levels on EPS formation and viability of Streptococcus mutans UA159 biofilms. Biofouling. 2015;31(7):555-63.
31. Melkam A, Sionov RV, Shalish M, et al. Enhanced Anti-Bacterial Activity of Arachidonic Acid against the Cariogenic Bacterium Streptococcus mutans in Combination with Triclosan and Fluoride. Antibiotics (Basel). 2024;13(6):540.
32. Magalhães TC, Lopes AG, Ferreira GF, et al. In vitro assessment of NaF/Chit supramolecular complex: Colloidal stability, antibacterial activity and enamel protection against S. mutans biofilm. J Dent. 2024;149(149):105316.